

The intrinsic collective X-ray spectrum of luminous high-mass X-ray binaries

S. Sazonov^{1,2*} and I. Khabibullin^{3,1}

¹Space Research Institute, Russian Academy of Sciences, Profsoyuznaya 84/32, 117997 Moscow, Russia

²Moscow Institute of Physics and Technology, Institutskiy per. 9, 141700 Dolgoprudny, Russia

³Max Planck Institute for Astrophysics, Karl-Schwarzschild-Strasse 1, D-85741 Garching, Germany

23 July 2018

ABSTRACT

Using a sample of two hundred luminous ($L_{X,\text{unabs}} > 10^{38}$ erg s⁻¹, where $L_{X,\text{unabs}}$ is the unabsorbed 0.25–8 keV luminosity) high-mass X-ray binary (HMXB) candidates found with *Chandra* in 27 nearby galaxies, we have constructed the collective X-ray spectrum of HMXBs in the local Universe per unit star formation rate, corrected for observational biases associated with intrinsic diversity of HMXB spectra and X-ray absorption in the interstellar medium. This spectrum is well fit by a power law with a photon index $\Gamma = 2.1 \pm 0.1$ and is dominated by ultraluminous X-ray sources with $L_{X,\text{unabs}} > 10^{39}$ erg s⁻¹. Hard sources (those with the 0.25–2 keV to 0.25–8 keV flux ratio of < 0.6) dominate above ~ 2 keV, while soft and supersoft sources (with the flux ratios of 0.6–0.95 and > 0.95 , respectively) at lower energies. The derived spectrum probably represents the angle-integrated X-ray emission of the near- and super-critically accreting stellar mass black holes and neutron stars in the local Universe. It provides an important constraint on supercritical accretion models and can be used as a reference spectrum for calculations of the X-ray preheating of the Universe by the first generations of X-ray binaries.

Key words: stars: black holes – accretion, accretion discs – X-rays: binaries – X-rays: galaxies – galaxies: star formation – early Universe

1 INTRODUCTION

The X-ray emission of actively star forming galaxies is dominated by the collective signal of high-mass X-ray binaries (HMXBs), complemented by diffuse soft X-ray emission from hot interstellar gas (e.g. Lehmer et al. 2010). Although the HMXB population of the Milky Way has been thoroughly studied (see Walter et al. 2015 for a recent review), the most luminous X-ray binaries are so rare that they can be found and counted only in other (nearby) galaxies. Such studies have revealed that the HMXB X-ray luminosity function (XLF) has a power-law shape: $dN/dL_X \propto L_X^{-1.6}$ from $L_X \lesssim 10^{36}$ to $\sim 10^{40}$ erg s⁻¹ (Mineo, Gilfanov, & Sunyaev 2012a), with some indication of steepening at $L_X \gtrsim 10^{40}$ erg s⁻¹. The bulk of the emission from point X-ray sources in actively star forming galaxies is thus produced by ultraluminous X-ray sources (ULXs) with $L_X \gtrsim 10^{39}$ erg s⁻¹, the majority of which appear to be supercritically accreting stellar-mass black holes (e.g. Poutanen et al. 2007; Feng & Soria 2011; Roberts et al. 2016) and neutron stars (Bachetti et al. 2014; Mushtukov et al. 2015; Fürst et al. 2016; Israel et al. 2017).

Luminous HMXBs, including ULXs and so-called ultraluminous supersoft sources (ULSs), exhibit a large variety of X-ray spectral shapes, probably due to differences in the accretion rate and orientation of the thick accretion disc with respect to the observer (e.g. Gladstone, Roberts, & Done 2009; Sutton, Roberts, & Middleton 2013; Urquhart & Soria 2016) as well as in the nature of the accretor (a neutron star vs. a black hole, Pintore et al. 2017). In addition, the observed X-ray spectra and detection rates of such objects can be significantly affected by photoabsorption in the interstellar medium (ISM) of the host galaxies and of the Milky Way. Taking all this into account, we have recently constructed (Sazonov & Khabibullin 2017a) the *intrinsic* HMXB XLF in its bright end, $10^{38} < L_{X,\text{unabs}} \lesssim 10^{40.5}$ erg s⁻¹ (where $L_{X,\text{unabs}}$ is the absorption corrected source luminosity in the 0.25–8 keV energy band), per unit star formation rate (SFR). It can be described by a power law, $dN/d\log L_{X,\text{unabs}} \approx 2.0(L_{X,\text{unabs}}/10^{39} \text{ erg s}^{-1})^{-0.6} (M_{\odot} \text{ yr}^{-1})^{-1}$, which has the same slope as the *observed* HMXB XLF of Mineo, Gilfanov, & Sunyaev (2012a) but a factor of ~ 2.3 higher normalization. We further showed that about two thirds of the total X-ray (0.25–8 keV) emission of HMXBs is released in the soft band (0.25–2 keV), $\sim 5 \times 10^{39}$ erg s⁻¹ ($M_{\odot} \text{ yr}^{-1}$)⁻¹, with

* E-mail: sazonov@iki.rssi.ru

roughly equal contributions from 'hard', 'soft' and 'super-soft' sources, defined according to their intrinsic soft/total X-ray flux ratio:

$$\begin{aligned} \text{Hard:} & \quad F_{0.25-2, \text{unabs}}/F_{0.25-8, \text{unabs}} \leq 0.6, \\ \text{Soft:} & \quad 0.6 < F_{0.25-2, \text{unabs}}/F_{0.25-8, \text{unabs}} \leq 0.95, \\ \text{Supersoft:} & \quad F_{0.25-2, \text{unabs}}/F_{0.25-8, \text{unabs}} > 0.95. \end{aligned} \quad (1)$$

This detailed information about the intrinsic XLF provides interesting constraints on the population properties of HMXBs and the physics of near- and super-critical accretion. It may also be interesting in the context of studying the 'cosmic dawn', since HMXBs belonging to the first generations of stars and their remnants might have radiatively preheated the Universe before it was reionized by UV radiation from stars and quasars (e.g. Mirabel et al. 2011). In our other recent paper (Sazonov & Khabibullin 2017b), we demonstrated (see also Madau & Fragos 2016) that HMXBs could significantly heat the Universe at $z \sim 10$ if the specific (i.e. per unit SFR) X-ray emissivity of such systems was higher by an order of magnitude than at the present epoch and the soft X-rays produced by HMXBs could escape from their host galaxies without strong attenuation in their ISM. Whether or not these conditions were fulfilled is an open question.

In Sazonov & Khabibullin (2017b) we used the measured ratio of the HMXB luminosity functions in the 0.25–2 and 0.25–8 keV bands to estimate the effective photon index of the average intrinsic X-ray spectrum of luminous HMXBs: $\Gamma \sim 2.1$. In the present study, we take advantage of the same sample of sources to construct the intrinsic (i.e. corrected for observational biases), SFR-normalized energy spectrum of the integrated emission of luminous HMXBs in the local Universe, hereafter referred to as the *intrinsic collective spectrum of HMXBs*, and evaluate the contributions of hard, soft and supersoft sources to it. This spectrum may find application, in particular, in simulations of the preheating of the early Universe by X-ray binaries.

2 SAMPLE

We make use of the 'clean sample' of X-ray sources detected by the *Chandra* X-ray Observatory (Wang et al. 2016), presumably located in 27 nearby ($D < 15$ Mpc) galaxies (mostly spirals), from Sazonov & Khabibullin (2017a). This sample had been compiled based on the following criteria: i) the source must be located on the sky within the 25 mag arcsec⁻² isophote of the galaxy, i.e. at radius $R < R_{25}$ in the plane of the galaxy, but outside of its central $0.05R_{25}$ region, ii) there must be at least 100 photon counts from the source in some *Chandra* observation and iii) the unabsorbed 0.25–8 keV luminosity of the source must exceed 10^{38} erg s⁻¹. Having additionally filtered out 16 known or suspected background active galactic nuclei (AGN) and 3 foreground Galactic stars, we had selected 200 HMXB candidates with luminosities ranging from $L_{X, \text{unabs}} = 10^{38}$ to $\sim 3 \times 10^{40}$ erg s⁻¹, and analyzed their *Chandra* spectra.

3 ANALYSIS

In Sazonov & Khabibullin (2017a), we described the measured spectrum of each source by one of the following models: i) absorbed power law, ii) absorbed blackbody emission and iii) absorbed multicolour blackbody disc emission. These best-fitting models were then used to determine the sources' intrinsic and observed luminosities in the 0.25–8 keV and 0.25–2 keV energy bands ($L_{X, \text{unabs}}$, $L_{X, \text{obs}}$, $L_{SX, \text{unabs}}$ and $L_{SX, \text{obs}}$, respectively). We now use the same spectral fits to determine the intrinsic and observed luminosities ($L_{i, \text{unabs}}$ and $L_{i, \text{obs}}$, respectively) in 5 narrow subbands: 0.25–0.5, 0.5–1, 1–2, 2–4, and 4–8 keV (hereafter referred to as bands $i = 1$ to 5).

Using high-quality maps of atomic (HI) and molecular (H₂) gas in the sampled galaxies, we demonstrated in Sazonov & Khabibullin (2017a) that the line-of-sight absorption column densities, N_{H} , inferred from the spectra of the studied X-ray sources (typically a few 10^{21} cm⁻²) can be attributed to the ISM of their host galaxies. We further took advantage of the HI, H₂ and SFR maps of the sampled galaxies to evaluate observational biases associated with the detection of X-ray sources by *Chandra*, which arise due to intrinsic diversity of HMXB spectra and X-ray absorption in the ISM. In a nutshell (see Sazonov & Khabibullin 2017a for a detailed discussion), in the absence of intervening absorbing gas, a soft source with a given intrinsic luminosity $L_{X, \text{unabs}}$ would produce more photon counts on the detector than a hard source with the same luminosity and location. On the other hand, observed X-ray fluxes of soft sources are more strongly affected by photoabsorption in the ISM, so that such sources may become hidden from *Chandra* if located on the farther side of their host galaxy. As a result, only some fraction of the total SFR ($\sim 32 M_{\odot} \text{ yr}^{-1}$) in the 27 sampled galaxies is effectively probed by *Chandra* in X-rays, and this fraction depends on the source intrinsic luminosity and spectral type, T : SFR ($L_{X, \text{unabs}}, T$) (Sazonov & Khabibullin 2017a).

In Sazonov & Khabibullin (2017a), we used the SFR ($L_{X, \text{unabs}}, T$) dependence to derive the HMXB XLF per unit SFR. We can now apply a similar procedure to construct the intrinsic collective spectrum of HMXBs in the local Universe by summation over the sources in the sample:

$$S_{i, \text{unabs}} = C_{\text{var}} \sum_j [1 - f_{\text{LMXB}}(L_{X, \text{unabs}, j})] \frac{L_{i, \text{unabs}, j}}{\text{SFR}(L_{X, \text{unabs}, j}, T_j)}. \quad (2)$$

Here, $S_{i, \text{unabs}}$ is the HMXB emissivity [measured in units of erg s⁻¹ ($M_{\odot} \text{ yr}^{-1}$)⁻¹] in energy band i (from 1 to 5), $L_{i, \text{unabs}, j}$ is the intrinsic luminosity in band i of the j th source, $L_{X, \text{unabs}, j}$ is its intrinsic 0.25–8 keV luminosity and T_j is its spectral type.

By means of equation (2), we perform a weighted stacking of the source spectra, such that each *Chandra* source provides a contribution equal to its luminosity in a given energy band divided by the corresponding X-ray-probed SFR. This procedure is analogous to the $1/V_{\text{max}}$ weighting method frequently used in astronomy, with SFR playing the role of a generalized V_{max} . Similar procedures have been used before e.g. for estimating the space density of stellar objects in the Galaxy taking into account their inhomogeneous spatial distribution (e.g. Tinney, Reid, & Mould 1993; Sazonov et al.

2006). Our current treatment also closely follows the calculation of the collective X-ray spectrum of AGN in the local Universe by Sazonov et al. (2008).

We have added two additional factors in equation (2). The factor $1 - f_{\text{LMXB}}(L_{X,\text{unabs},j})$ takes into account that our sample of HMXB candidates is expected to be contaminated by low-mass X-ray binaries (LMXBs). Their relative contribution as a function of luminosity was estimated in Sazonov & Khabibullin (2017a) based on the LMXB XLF (Gilfanov 2004) and can be approximated as

$$f_{\text{LMXB}} = \begin{cases} 0.49, & 10^{38} \leq L_{X,\text{unabs}} < 10^{38.5} \text{ erg s}^{-1}, \\ 0.41, & 10^{38.5} \leq L_{X,\text{unabs}} < 10^{39} \text{ erg s}^{-1}, \\ 0.06, & 10^{39} \leq L_{X,\text{unabs}} < 10^{39.5} \text{ erg s}^{-1}, \\ 0, & L_{X,\text{unabs}} \geq 10^{39.5} \text{ erg s}^{-1}. \end{cases} \quad (3)$$

The LMXB contribution is thus substantial below $10^{39} \text{ erg s}^{-1}$ but negligible at higher luminosities. Therefore, since most of the emission from HMXBs is produced by ULXs (with $L_{X,\text{unabs}} > 10^{39} \text{ erg s}^{-1}$), the significant uncertainty in our knowledge of the LMXB XLF and hence their contribution to our sample does not translate into a significant uncertainty in the resulting collective spectrum of HMXBs.

The additional coefficient $C_{\text{var}} = 1/1.2 \approx 0.83$ in equation (2) takes into account the 'variability bias' evaluated in Sazonov & Khabibullin (2017a). It results from our using particular *Chandra* observations for estimating the luminosities of the sources (namely those with at least 100 counts from the source) while the same sources would be weaker by $\sim 20\%$ on average due to intrinsic variability if their luminosities were measured randomly in time.

There are two types of uncertainties associated with the collective spectrum $S_{i,\text{unabs}}$. One is due to uncertainties, $\delta L_{i,\text{unabs},j}$, in estimation of the unabsorbed luminosities of the individual sources from X-ray spectral analysis:

$$\delta_{i,1} = C_{\text{var}} \sqrt{\sum_j \left([1 - f_{\text{LMXB}}(L_{X,\text{unabs},j})] \frac{\delta L_{i,\text{unabs},j}}{\text{SFR}(L_{X,\text{unabs},j}, T_j)} \right)^2}. \quad (4)$$

Another arises from the finite size of our source sample:

$$\delta_{i,2} = C_{\text{var}} \sqrt{\sum_j \left([1 - f_{\text{LMXB}}(L_{X,\text{unabs},j})] \frac{L_{i,\text{unabs},j}}{\text{SFR}(L_{X,\text{unabs},j}, T_j)} \right)^2}. \quad (5)$$

This uncertainty stems from the fact that in the standard $\sum 1/V_{\text{max},j}$ estimation of space densities, the uncertainty of each object's contribution is assumed to follow Poisson statistics (Felten 1976) so that the variance of the density estimate is $\sum 1/V_{\text{max},j}^2$ (e.g. Tinney, Reid, & Mould 1993). In our case, the contributions of individual sources to the variance of $S_{i,\text{unabs}}$ are similarly independent of each other but must be multiplied by the square of the corresponding coefficients in equation (2).

The total uncertainty can be estimated as a combination of these uncertainties:

$$\delta_i = \sqrt{\delta_{i,1}^2 + \delta_{i,2}^2}. \quad (6)$$

We can use a slightly modified stacking procedure to also compute the *observed* collective spectrum of HMXBs

in the local Universe:

$$S_{i,\text{obs}} = C_{\text{var}} \sum_j [1 - f_{\text{LMXB}}(L_{X,\text{unabs},j})] \frac{L_{i,\text{obs},j}}{\text{SFR}(L_{X,\text{unabs},j}, T_j)}. \quad (7)$$

This spectrum represents the integrated X-ray emission of HMXBs as seen by the Earth's observer, i.e. uncorrected for line-of-sight absorption. In this case, the uncertainties of the first type are negligible due to the small $\delta L_{i,\text{obs},j}$ errors and those of the second type can be computed using equation (5) by substituting $L_{i,\text{obs},j}$ for $L_{i,\text{unabs},j}$.

4 RESULTS

4.1 Intrinsic spectrum

Figure 1 shows the *intrinsic* collective spectrum of HMXBs with $10^{38} < L_{X,\text{unabs}} \leq 10^{40.5} \text{ erg s}^{-1}$ (the luminosity range spanned by our sample of sources), obtained using equation (2). It can be well fitted ($\chi^2 = 0.21$ for 3 degrees of freedom) by a power law:

$$\frac{EL_E}{\text{SFR}} = (2.1 \pm 0.4) \times 10^{39} \left(\frac{E}{\text{keV}} \right)^{-0.11 \pm 0.18} \text{ erg s}^{-1} (M_{\odot} \text{ yr})^{-1}. \quad (8)$$

The quoted uncertainty for the spectral slope may be slightly overestimated because we regard the uncertainties δ_i of the individual spectral points as independent, although they may be somewhat correlated due to the contribution $\delta_{i,2}$ [eq. (5)] from the Poisson uncertainty in the number of sampled sources (this is only important for the three higher energy channels, since the uncertainties in the 0.25–0.5 keV and 0.5–1 keV bands are dominated by the $\delta_{i,1}$ errors associated with luminosity estimation for individual sources).

As could be expected from the HMXB XLF (Sazonov & Khabibullin 2017a), the bulk of the emission from HMXBs is provided by ultraluminous ($L_{X,\text{unabs}} > 10^{39} \text{ erg s}^{-1}$) sources (see Fig. 1). Moreover, there is an indication that a sizeable or even dominant contribution is provided by extremely luminous sources with $L_{X,\text{unabs}} > 10^{40} \text{ erg s}^{-1}$. These results are unlikely to be strongly affected by LMXB contamination of our sample of sources, which we have roughly taken into account through the $1 - f_{\text{LMXB}}$ factor in equation (2). Indeed, LMXBs are only important at $L_{X,\text{unabs}} < 10^{39} \text{ erg s}^{-1}$, but the overall contribution of such relatively low-luminosity sources to the total emission from HMXBs is small, while nearly all of our $L_{X,\text{unabs}} > 10^{39} \text{ erg s}^{-1}$ sources are expected to be HMXBs.

The large uncertainties of the collective spectrum of HMXBs in the two softest bands are mainly associated with the presence of two very luminous ($L_{X,\text{unabs}} \geq 10^{40} \text{ erg s}^{-1}$) supersoft [per our definition, eq. (1)] sources in our sample. As discussed in Sazonov & Khabibullin (2017a), these sources have very soft spectra (which can be described as blackbody radiation with $kT_{\text{bb}} \sim 0.06\text{--}0.07 \text{ keV}$) and their inferred intrinsic luminosities are some 3 orders of magnitude higher than their observed luminosities (apparently due to the presence of significant amounts of cold ISM in their direction) but very uncertain (by 1–2 orders of magnitude). Moreover, there are in total only 7 sources (2 hard, 3 soft and 2 supersoft ones) with $L_{X,\text{unabs}} > 10^{40} \text{ erg s}^{-1}$ in our sample, so that the overall contribution of such luminous sources to the total X-ray emission produced by HMXBs is not well constrained by the present study.

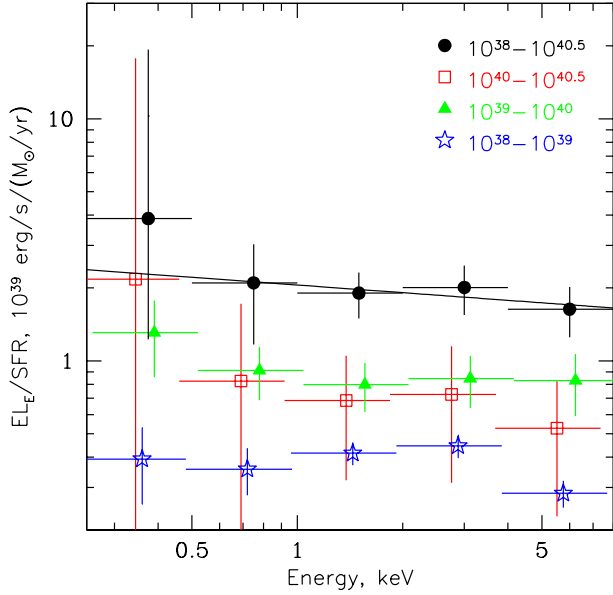


Figure 1. Intrinsic collective spectrum of HMXBs in the local Universe (black circles) and the contributions (these points are slightly shifted along the horizontal axis for better visibility) of sources in three luminosity ranges: $L_{X,\text{unabs}} = 10^{40}\text{--}10^{40.5}$ erg s $^{-1}$ (red squares), $10^{39}\text{--}10^{40}$ erg s $^{-1}$ (green triangles) and $10^{38}\text{--}10^{39}$ erg s $^{-1}$ (blue stars). The solid line is the best-fitting power law for the total spectrum [eq. (8)].

Given the large uncertainty associated with the contribution of the most luminous sources ($L_{X,\text{unabs}} > 10^{40}$ erg s $^{-1}$), we also calculated the collective spectrum of HMXBs with $10^{38} < L_{X,\text{unabs}} < 10^{40}$ erg s $^{-1}$ (there are in total 193 such objects in our sample), which is shown in Fig. 2. This spectrum is tightly constrained and can be well fitted ($\chi^2 = 0.71$ for 3 degrees of freedom) by the following power law:

$$\frac{EL_E}{\text{SFR}} = (1.31 \pm 0.13) \times 10^{39} \left(\frac{E}{\text{keV}}\right)^{-0.08 \pm 0.11} \text{ erg s}^{-1} (M_{\odot} \text{ yr})^{-1}. \quad (9)$$

Comparing this expression with equation (8) we see that the slope is unchanged, but the normalization has decreased by $\sim 20\text{--}50\%$, which reflects the substantial contribution of the most luminous ($L_{X,\text{unabs}} \geq 10^{40}$ erg s $^{-1}$) sources to the total X-ray emission from HMXBs. The derived spectral slope (photon index) $\Gamma \approx 2.1$ confirms the conclusion of our previous work (Sazonov & Khabibullin 2017a,b) that about two thirds of the total X-ray output of HXMBs emerges in the form of soft X-rays, at energies below 2 keV.

Although the shape of the collective spectrum of HMXBs is consistent with a simple power law, this is merely the result of summing over a great variety of individual spectra. In reality, as shown in Fig. 2, hard, soft and supersoft sources (again, per our definition) provide comparable contributions to the total spectrum, and it is the soft and supersoft sources that are largely responsible for its low-energy part. The presented collective spectra of the hard, soft and supersoft sources have been obtained using the same stacking procedure [eq. (2)] as for the total spectrum, applied to 117, 47 and 29 sources of these classes, respectively (excluding the 7 sources with $L_{X,\text{unabs}} > 10^{40}$ erg s $^{-1}$). These spectra

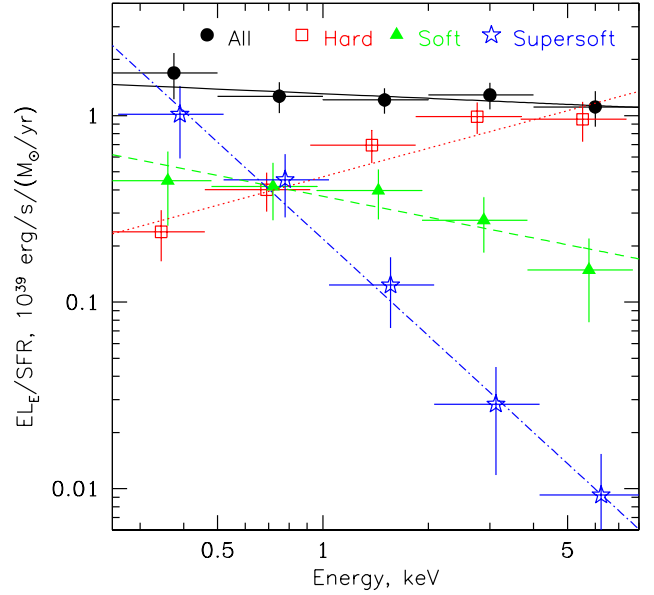


Figure 2. Intrinsic collective spectrum of HMXBs with $10^{38} < L_{X,\text{unabs}} < 10^{40}$ erg s $^{-1}$ per unit SFR (black circles) and the contributions of hard, soft and supersoft sources [according to our definition, eq. (1)]: squares, triangles and stars, respectively. The black solid line shows the best-fitting power law for the total spectrum [eq. (9)]. The red dotted, green dashed and blue dash-dotted lines show the corresponding fits for the hard, soft and supersoft components [eqs. (10), (11) and (12), respectively].

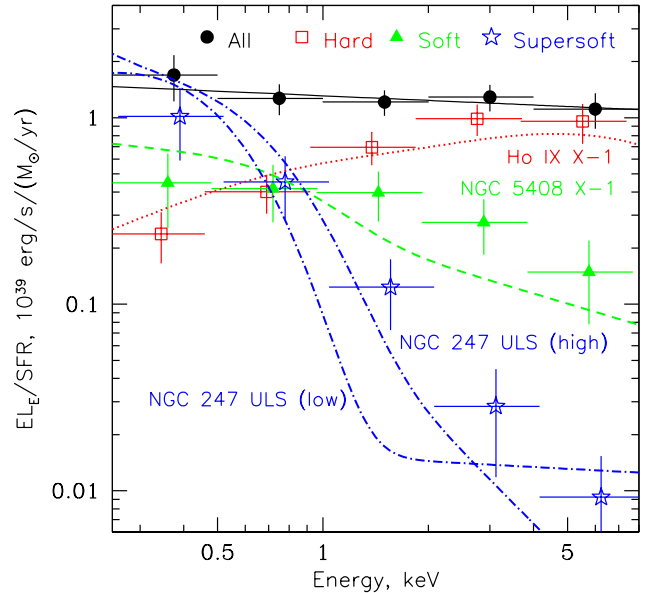


Figure 3. Same as Fig. 2, but the power-law fits for hard, soft and supersoft sources are replaced by examples of spectra (best-fitting unabsorbed models) of real individual sources (with ad hoc normalizations) of real individual sources belonging to these categories: red dotted line – ULX Ho IX X-1, green dashed line – ULX NGC 5408 X-1, blue dash-dotted lines – NGC 247 ULS in two different states (see references in the text). None of these sources belong to our sample.

can be well fitted ($\chi^2 = 2.79$, 1.06 and 0.63, respectively, for 3 degrees of freedom) by the following power laws:

$$\left(\frac{EL_E}{\text{SFR}}\right)_{\text{hard}} = (0.47 \pm 0.05) \times 10^{39} \left(\frac{E}{\text{keV}}\right)^{0.51 \pm 0.10} \text{ erg s}^{-1} (M_{\odot} \text{ yr})^{-1}. \quad (10)$$

$$\left(\frac{EL_E}{\text{SFR}}\right)_{\text{soft}} = (0.37 \pm 0.06) \times 10^{39} \left(\frac{E}{\text{keV}}\right)^{-0.37 \pm 0.16} \text{ erg s}^{-1} (M_{\odot} \text{ yr})^{-1}. \quad (11)$$

$$\left(\frac{EL_E}{\text{SFR}}\right)_{\text{supersoft}} = (0.22 \pm 0.09) \times 10^{39} \left(\frac{E}{\text{keV}}\right)^{-1.72 \pm 0.21} \text{ erg s}^{-1} (M_{\odot} \text{ yr})^{-1}. \quad (12)$$

In reality our partition of HMXBs into three classes is ad hoc, and each of these groups exhibits significant diversity of individual source spectra (see the best-fitting spectral parameters for our sources in Sazonov & Khabibullin 2017a). Nevertheless, the collective spectra for these classes allow for some generalizing description.

First, the collective spectrum of hard sources resembles typical, hard spectra of ULXs in the so-called 'broadened-disc' and 'hard ultraluminous' states introduced by Sutton, Roberts, & Middleton (2013). To demonstrate this, we show in Fig. 3 the best-fitting (unabsorbed) model (Sazonov, Lutovinov, & Krivonos 2014, their table 2) for an X-ray spectrum of the well-known ULX Ho IX X-1 taken by the XMM-Newton observatory (observation 0657801801), which consists of i) a hard ($\Gamma = 1.28$) power-law component with a high-energy exponential cutoff at $E_{\text{cut}} = 6.4$ keV and ii) a weak additional, multicolour blackbody disc emission component with $kT_{\text{in}} = 0.3$ keV (*cutoffpl+diskbb* in XSPEC, Arnaud 1996). We see that this spectrum nearly matches our collective spectrum of hard sources.

Also shown in Fig. 3 is the best-fitting model (Sutton, Roberts, & Middleton 2013, their table A1) for an XMM-Newton spectrum of NGC 5408 X-1, which according to the classification scheme of these authors is a representative of the so-called 'soft ultraluminous' ULX spectral class. In this case, the spectrum consists of a fairly steep power-law component with $\Gamma = 2.56$ and a multicolour blackbody component with $kT_{\text{in}} = 0.194$ keV (*powerlaw+diskbb*). This spectrum is fairly similar, although not an exact match, to our collective spectrum of soft sources.

As for the spectra of our supersoft sources, most of them can be described in terms of blackbody emission with kT_{bb} ranging from ~ 0.05 to ~ 0.25 keV or multicolour disc emission with kT_{in} ranging from ~ 0.1 to ~ 0.3 keV, although the spectra of 5 supersoft sources are somewhat better described by a power law with $\Gamma \sim 3.4$ – 3.8 (see Sazonov & Khabibullin 2017a). Hence, the softer spectra in this category are similar to typical ULS spectra (Di Stefano & Kong 2003; Urquhart & Soria 2016) while the harder ones resemble the spectra of 'normal' X-ray binaries in high/soft states associated with high but subcritical accretion rates (see Done, Gierliński, & Kubota 2007 for a review). Among our lowest luminosity ($10^{38} < L_{X,\text{unabs}} \leq 2 \times 10^{38}$ erg s $^{-1}$) supersoft sources there may also be present classical supersoft sources associated with accreting white dwarfs (e.g. Soraisam et al. 2016), but such objects are not expected to provide a significant contribution to the collective spectrum of HMXBs, according to the HMXB XLF obtained in Sazonov & Khabibullin (2017a).

Some or most of the harder spectra in the supersoft cat-

egory may correspond to intermediate states between the supersoft ultraluminous state typical of ULXs and the soft ultraluminous state occurring in ULXs (see above). In fact, there is growing evidence that ultraluminous sources can make transitions between these states. One example of such behaviour is shown in Fig. 3 based on the study by Feng et al. (2016): NGC 247 ULS has been observed by *Chandra* and *XMM-Newton* to switch between i) a 'low', supersoft ultraluminous state, when its spectrum is dominated by soft thermal emission ($kT_{\text{in}} = 0.11$ keV) but exhibits an additional, weak power-law component ($\Gamma = 2.1 \pm 0.9$, here we use the parameters for the *diskbb+powerlaw* model from table 3 of Feng et al. 2016), which dominates above ~ 2 keV, and ii) a 'high' state, when the thermal component is somewhat harder ($kT_{\text{in}} = 0.15$ keV) and the power-law ($\Gamma = 3.9 \pm 0.4$) component provides a larger contribution to the X-ray luminosity¹. The latter state appears to be intermediate between the supersoft and soft ultraluminous states. A similar spectral transition has been observed in the well-known ULS in M101 (Soria & Kong 2016). We see from Fig. 3 that our collective spectrum of supersoft sources may well be a superposition of spectra corresponding to different states of ULXs.

We conclude that the collective spectrum of HMXBs can be described in terms of a superposition of different (known) spectral states of near- and super-critically accreting X-ray binaries, which probably reflect differences in the accretion rate and inclination of the accretion disc with respect to the observer (see a further discussion in §5 below).

4.2 Observed spectrum

Figure 4 shows the *observed* collective spectrum of HMXBs, obtained using equation (7) by stacking the weighted spectra of all 200 sources in the sample ($10^{38} < L_{X,\text{unabs}} < 10^{40.5}$ erg s $^{-1}$). As demonstrated in the figure, the observed spectrum is dominated by hard sources, with the contributions of soft and especially supersoft sources being significantly suppressed compared to the intrinsic spectrum as a result (mainly) of attenuation of their emission in the ISM of their host galaxies (see Sazonov & Khabibullin 2017a). This effect is only noticeable below 2 keV. The observed spectrum can be approximately described as the intrinsic spectrum [a power law with $\Gamma = 2.1$, see eqs. (8), (9)] absorbed in cold gas with column density $N_{\text{H}} = (1.2 \pm 0.2) \times 10^{21}$ cm $^{-2}$ (see Fig. 4). This value is very close to the median absorption column of 1.1×10^{21} cm $^{-2}$ for our sample of sources, inferred from their X-ray spectra (Sazonov & Khabibullin 2017a).

It is interesting to compare the observed collective spectrum of HMXBs constructed here with observed galaxy-wide X-ray spectra of actively star forming galaxies. Several such spectra, measured with *Chandra* and *NuSTAR*, have been presented by Lehmer et al. (2015), of which the most interesting is that of the starburst galaxy NGC 3256. This galaxy has a very high total SFR of $\sim 36 M_{\odot} \text{ yr}^{-1}$, which is similar to the combined SFR of all 27 galaxies making up our sample ($\sim 32 M_{\odot} \text{ yr}^{-1}$). Therefore, NGC 3256 should be as

¹ We have neglected an additional, weak component representing thermal emission from an optically thin plasma in the best-fitting model of Feng et al. (2016) for NGC 247 ULS in its high state.

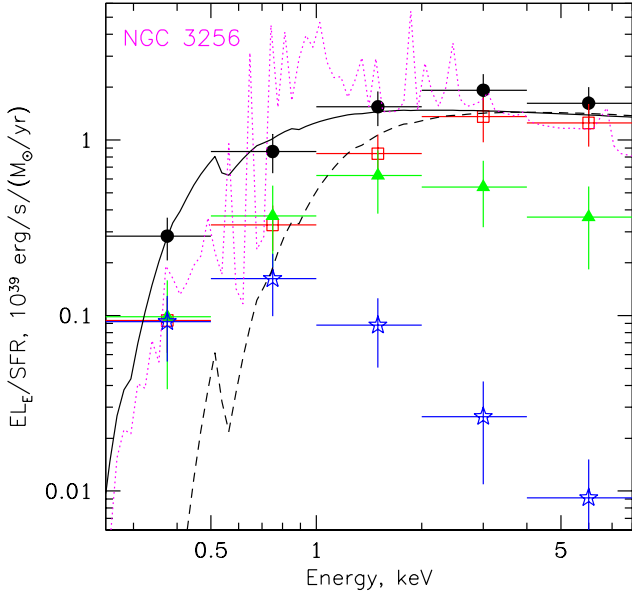


Figure 4. Observed collective spectrum of HMXBs ($10^{38} < L_{X,\text{unabs}} < 10^{40.5}$ erg s $^{-1}$) (black circles) and the contributions of hard, soft and supersoft sources (squares, triangles and stars, respectively). The black solid line shows the best-fitting absorbed power-law model for the total spectrum, with a photon index fixed at $\Gamma = 2.1$ (as inferred for the intrinsic HMXB spectrum) and $N_{\text{H}} = 1.2 \times 10^{21}$ cm $^{-2}$. The magenta dotted line shows the observed SFR-normalized X-ray spectrum of the NGC 3256 starburst galaxy (Lehmer et al. 2015). The black dashed line shows our intrinsic collective spectrum of HMXBs absorbed by $N_{\text{H}} = 5 \times 10^{21}$ cm $^{-2}$ of cold gas, which is a crude estimate (based on the atomic and molecular gas content of this galaxy, see text) of the typical ISM column density towards the HMXBs in NGC 3256.

representative of the local luminous HMXB population as our sample of galaxies.

As shown in Fig. 4, the SFR-normalized spectrum of NGC 3256 nearly matches our observed collective spectrum of HMXBs at energies above ~ 3 keV, confirming that the total emission of actively star forming galaxies at these energies is dominated by ULXs. It is more difficult to compare the collective spectrum of HMXBs and the NGC 3256 spectrum below 3 keV. First, as discussed by Lehmer et al. (2015) and evident from the strong X-ray line emission observed from NGC 3256, thermal emission from hot interstellar gas provides a strong contribution to the soft X-ray flux from this galaxy. Secondly, soft X-ray emission from point sources in NGC 3256 can be significantly suppressed by absorption in the cold component of its ISM, in fact much stronger than for typical galaxies in our sample, which are characterized by much lower SFRs (at most $\sim 3 M_{\odot}$ yr $^{-1}$) and smaller amounts of cold gas.

We can roughly estimate the expected absorption column density for the X-ray sources in NGC 3256 using measurements of its total gas content and assuming that the gas is uniformly distributed over a disc of some characteristic radius R . For the atomic gas, the total mass is estimated as $M_{\text{HI}} \sim 6 \times 10^9 M_{\odot}$, with $R_{\text{HI}} \sim 30$ kpc (e.g. Casasola, Bettoni, & Galletta 2004), while for the molecular gas $M_{\text{H}_2} \sim 5 \times 10^9 M_{\odot}$ with $R_{\text{H}_2} \sim 6.6$ kpc (Ueda et al. 2014). This yields integrated

column densities (perpendicular to the plane of the galaxy) of $N_{\text{H}} \sim 3 \times 10^{20}$ and $\sim 5 \times 10^{21}$ cm $^{-2}$ for the atomic and molecular gas, respectively. Taking into account that NGC 3256 is inclined at $\sim 48^{\circ}$ (according to HyperLeda²) to our line of sight and the Galactic absorption of $\sim 7 \times 10^{20}$ cm $^{-2}$ in its direction (Kalberla et al. 2005), we infer that X-ray sources in this galaxy should typically be screened from us by $N_{\text{H}} \sim 5 \times 10^{21}$ cm $^{-2}$ of cold gas. Subjecting our intrinsic ($\Gamma = 2.1$) collective spectrum of HMXBs to this amount of absorption results in a spectrum shown in Fig. 4. We see that most of the soft X-ray emission produced by the HMXBs in NGC 3256 can be obscured by the ISM. In reality, HMXBs are usually concentrated to regions of active star formation and enhanced gas column density, so the ensemble-averaged N_{H} for the HMXB population of NGC 3256 can be even higher than in our estimate.

Comparison of Fig. 1 and Fig. 4 suggests that the (mostly obscured) population of luminous soft HMXBs in NGC 3256 probably produces a similar amount of soft X-rays as its hot interstellar gas. This is in agreement with the conclusion reached by Mineo, Gilfanov, & Sunyaev (2012a,b), who compared the integrated contributions of point X-ray sources and hot ISM to the galaxy-wide X-ray luminosity for two dozens of nearby galaxies and found both contributions to be similar and proportional to the SFR, albeit within a large uncertainty associated with cold-gas absorption of soft X-rays emitted by hot gas. According to the linear relation found by Mineo, Gilfanov, & Sunyaev (2012b), the intrinsic X-ray (0.3–10 keV) luminosity of the ISM of a galaxy with a given SFR is expected to be $\sim 7 \times 10^{39}$ (SFR/ M_{\odot} yr $^{-1}$) erg s $^{-1}$. Taking into account the substantial intrinsic absorption in NGC 3256 (see the discussion above) it appears from Fig. 4 that NGC 3256 is consistent with the Mineo, Gilfanov, & Sunyaev (2012b) correlation.

The apparent approximate parity between the total X-ray outputs of the luminous HMXB population and hot ISM in star forming galaxies is interesting and should be further studied in future work.

5 DISCUSSION

Although the exact nature of the sources comprising our sample is unknown, we have demonstrated that the intrinsic collective spectrum of HMXBs can be described in terms of a superposition of various known spectral states of luminous X-ray binaries: the broadened-disc, hard ultraluminous and soft ultraluminous states known for ULXs (Sutton, Roberts, & Middleton 2013), the very soft ($T_{\text{bb}} \sim 0.1$ keV) blackbody-like state typical of ULs (Urquhart & Soria 2016) and the high/soft states of ‘normal’ X-ray binaries (Done, Gierliński, & Kubota 2007). All these states may be different manifestations of near- or super-critical accretion of matter from a massive stellar companion onto a stellar-mass black hole (or a neutron star in some systems), reflecting differences in the accretion rate and/or in the orientation of the (thick) accretion disc and its wind with respect to the observer (e.g. Middleton et al. 2015; Feng et al. 2016; Gu et al. 2016; Urquhart & Soria 2016). The basic idea discussed in these

² <http://leda.univ-lyon1.fr/>

recent papers is that when the disc is observed nearly face-on, (relatively) hard X-ray radiation from the central funnel is directly visible. However, the central emission region can be obscured by the wind from an observer viewing the disc at larger inclination, so that only reprocessed softer emission will be visible.

Kawashima et al. (2012) have performed a detailed modelling of X-ray spectra generated by supercritical accretion onto a stellar-mass black hole, combining the results of hydrodynamical simulations of a thick accretion flow with Monte-Carlo radiative transfer in this flow. The findings of this work are in good agreement with the general picture adopted in the aforementioned studies, namely the appearance of a supercritical accretor should strongly depend on the viewing angle: the source will appear more luminous and harder if observed face-on and weaker and softer if observed at a large angle. According to the angular dependence of the observed X-ray luminosity (for a given accretion rate) obtained by Kawashima et al. (2012) (see their fig. 3), objects viewed at intermediate angles of $i \sim 10\text{--}40^\circ$ should dominate in the collective X-ray emission of the local population of supercritical accretors (assuming, of course, that they are randomly oriented). Therefore, the angle-integrated spectrum of such sources should be somewhat softer than the spectra of face-on ($i = 0$) objects, namely it is expected to have an effective photon index of $\Gamma \sim 2$ according to fig. 4 in Kawashima et al. (2012). This value is close to the $\Gamma = 2.1 \pm 0.1$ slope of our collective spectrum of luminous HMXBs, demonstrating that this spectrum (as well as its composition in terms of sources of different luminosities and spectral types) places interesting observational constraints on supercritical accretion models.

The present study suggests that the average spectral hardness of luminous HMXBs does not strongly depend on their luminosity (compare the collective spectra for three different luminosity bins in Fig. 1), which seems to contradict the general picture outlined above, according to which spectral hardness should positively correlate with the observed luminosity of ULXs. Part of the explanation why the collective spectrum of our least luminous ($L_{X,\text{unabs}} = 10^{38}\text{--}10^{39} \text{ erg s}^{-1}$) sources is as hard as the spectra of more luminous objects may be that this low-luminosity bin probably includes, apart from (soft) supercritical accretors, sub- and near-critically accreting black holes and neutron stars with relatively hard spectra. Another reason may be that the spectrum for this luminosity bin is significantly affected by LMXB contamination, which we have roughly taken into account [via eq. (3)] for the normalization but not for the shape of the spectrum.

According to the collective spectrum of HMXBs, soft X-ray emission (0.25–2 keV) dominates the total radiative output of HMXBs in the local Universe. This fact has been frequently overlooked in previous studies, because much of this soft X-ray emission is absorbed in the ISM and does not reach the Earth’s absorber. The lower energy boundary of 0.25 keV in our analysis is mainly set by the sensitivity of the *Chandra* X-ray telescope. What if the collective spectrum of HMXBs continues with nearly the same slope ($\Gamma = 2.1$) to yet lower energies? This would mean that the luminous HMXB population produces, apart from X-rays, a comparable or even higher luminosity, $\gtrsim 5 \times 10^{39} \text{ erg s}^{-1} (M_\odot \text{ yr}^{-1})^{-1}$, at UV and lower frequencies. This hidden radiation, if real, may be

associated with ‘misaligned ULXs’, i.e. supercritically accreting massive binaries viewed at yet higher inclinations and/or having yet higher accretion rates than ULXs and ULSS, and the famous Galactic microquasar SS 433 may be one of such systems (e.g. Fabrika 2004; Poutanen et al. 2007; Khabibullin & Sazonov 2016). Indeed, the observed (albeit only at $E \gtrsim 2$ keV, because of strong line-of-sight absorption in the soft band) X-ray luminosity of SS 433 is only $\sim 10^{36} \text{ erg s}^{-1}$ (and it is associated with its baryonic jets rather than directly with the central source), while its UV luminosity is estimated as $\sim 10^{40}\text{--}10^{41} \text{ erg s}^{-1}$ (Cherepashchuk, Aslanov, & Kornilov 1982; Dolan et al. 1997), and this radiation is probably associated with the photosphere of the disc wind (Fabrika 2004).

6 CONCLUSION

Using a sample of 200 luminous ($L_{X,\text{unabs}} > 10^{38} \text{ erg s}^{-1}$) HMXB candidates detected by *Chandra* in 27 nearby galaxies, we have constructed the collective X-ray spectrum of HMXBs in the local Universe per unit star formation rate, corrected for observational biases associated with intrinsic diversity of source spectra and X-ray absorption in the ISM (of the host galaxies and the Milky Way). This spectrum can be described by a power law with a photon index $\Gamma = 2.1 \pm 0.1$ [eqs. (8) and (9)] and is dominated by ultraluminous sources ($L_{X,\text{unabs}} > 10^{39} \text{ erg s}^{-1}$), with comparable contributions from hard, soft and supersoft sources [as defined in eq. (1)]. Hard sources, whose spectra resemble those of ‘classical’ ULXs, dominate at energies above a few keV, while the bulk of the soft X-ray emission (below 2 keV) is provided by soft and supersoft sources.

If our favoured interpretation that the derived spectrum mainly represents population- and angle-integrated emission from supercritically accreting HMXBs is correct, then its nearly flat shape (in νF_ν units) provides an interesting constraint on theoretical models of supercritical accretion.

The strong soft X-ray emission revealed by the intrinsic collective spectrum of HMXBs could play an important role in the early Universe, since the ISM in the first galaxies was probably more transparent to X-rays than in present-day galaxies, in particular due to the lower metallicity of the former. As a result, soft and supersoft luminous HMXBs might have been the key contributors to the X-ray heating of the Universe prior to its reionization, as we have discussed recently (Sazonov & Khabibullin 2017b). The collective spectrum of HMXBs obtained here can thus be used as a reference spectrum for detailed simulations of cosmic X-ray preheating.

ACKNOWLEDGMENTS

The authors thank the referee for useful suggestions.

REFERENCES

- Arnaud K. A., 1996, ASPC, 101, 17
- Bachetti M., et al., 2014, *Natur*, 514, 202
- Casasola V., Bettoni D., Galletta G., 2004, *A&A*, 422, 194

- Cherepashchuk A. M., Aslanov A. A., Kornilov V. G., 1982, SvA, 26, 697
- Di Stefano R., Kong A. K. H., 2003, ApJ, 592, 884
- Dolan J. F., et al., 1997, A&A, 327, 648
- Done C., Gierliński M., Kubota A., 2007, A&ARv, 15, 1
- Fabrika S., 2004, ASPRv, 12, 1
- Felten J. E., 1976, ApJ, 207, 700
- Feng H., Soria R., 2011, NewAR, 55, 166
- Feng H., Tao L., Kaaret P., Grisé F., 2016, ApJ, 831, 117
- Fürst F., et al., 2016, ApJ, 831, L14
- Gilfanov M., 2004, MNRAS, 349, 146
- Gladstone J. C., Roberts T. P., Done C., 2009, MNRAS, 397, 1836
- Gu W.-M., Sun M.-Y., Lu Y.-J., Yuan F., Liu J.-F., 2016, ApJ, 818, L4
- Israel G. L., et al., 2017, MNRAS, 466, L48
- Kalberla P. M. W., Burton W. B., Hartmann D., Arnal E. M., Bajaja E., Morras R., Pöppel W. G. L., 2005, A&A, 440, 775
- Kawashima T., Ohsuga K., Mineshige S., Yoshida T., Heinzeller D., Matsumoto R., 2012, ApJ, 752, 18
- Khabibullin I., Sazonov S., 2016, MNRAS, 457, 3963
- Lehmer B. D., Alexander D. M., Bauer F. E., Brandt W. N., Goulding A. D., Jenkins L. P., Ptak A., Roberts T. P., 2010, ApJ, 724, 559
- Lehmer B. D., et al., 2015, ApJ, 806, 126
- Madau, P., & Fragos, T., arXiv:1606.07887
- Middleton M. J., Heil L., Pintore F., Walton D. J., Roberts T. P., 2015, MNRAS, 447, 3243
- Mineo S., Gilfanov M., Sunyaev R., 2012a, MNRAS, 419, 2095
- Mineo S., Gilfanov M., Sunyaev R., 2012b, MNRAS, 426, 1870
- Mirabel I. F., Dijkstra M., Laurent P., Loeb A., Pritchard J. R., 2011, A&A, 528, A149
- Mushtukov A. A., Suleimanov V. F., Tsygankov S. S., Poutanen J., 2015, MNRAS, 454, 2539
- Pintore F., Zampieri L., Stella L., Wolter A., Mereghetti S., Israel G. L., 2017, arXiv, arXiv:1701.03595
- Poutanen J., Lipunova G., Fabrika S., Butkevich A. G., Abolmasov P., 2007, MNRAS, 377, 1187
- Roberts T. P., Middleton M. J., Sutton A. D., Mezcuca M., Walton D. J., Heil L. M., 2016, AN, 337, 534
- Sazonov S., Revnivtsev M., Gilfanov M., Churazov E., Sunyaev R., 2006, A&A, 450, 117
- Sazonov S., Krivonos R., Revnivtsev M., Churazov E., Sunyaev R., 2008, A&A, 482, 517
- Sazonov S. Y., Lutovinov A. A., Krivonos R. A., 2014, AstL, 40, 65
- Sazonov S., Khabibullin I., 2017a, MNRAS, 466, 1019
- Sazonov S., Khabibullin I., 2017b, Astron. Lett., 43, 243
- Soraisam M. D., Gilfanov M., Wolf W. M., Bildsten L., 2016, MNRAS, 455, 668
- Soria R., Kong A., 2016, MNRAS, 456, 1837
- Sutton A. D., Roberts T. P., Middleton M. J., 2013, MNRAS, 435, 1758
- Tinney C. G., Reid I. N., Mould J. R., 1993, ApJ, 414, 254
- Ueda J., et al., 2014, ApJS, 214, 1
- Urquhart R., Soria R., 2016, MNRAS, 456, 1859
- Walter R., Lutovinov A. A., Bozzo E., Tsygankov S. S., 2015, A&ARv, 23, 2
- Wang S., Liu J., Qiu Y., Bai Y., Yang H., Guo J., Zhang P., 2016, ApJS, 224, 40

This paper has been typeset from a $\text{\TeX}/\text{\LaTeX}$ file prepared by the author.